Journal of Coupled Systems and Multiscale Dynamics

doi:10.1166/jcsmd.2015.1081
J. Coupled Syst. Multiscale Dyn.
Vol. 3(3)/2330-152X/2015/228/005

Research Article

Local magnetic field perturbations caused by magnetic susceptibility heterogeneity in myelin-water layers within an axon

Bradley J. Roth[1,*], Steffan Puwal[1], and Peter J. Basser[2]

[1]*Department of Physics, Oakland University, Rochester, Michigan 48309, USA*
[2]*Eunice Kennedy Shriver National Institute of Child Health and Human Development, National Institutes of Health, Bethesda, Maryland 20892, USA*

(Received: 8 December 2014. Accepted: 20 March 2015)

ABSTRACT

Magnetic resonance imaging has been used to map the myelin water fraction in neural tissue. One hypothesis is that a reduction in T_2^* arises from microscopic perturbations in the magnetic field caused by heterogeneities in the magnetic susceptibility of myelin. In this paper, the perturbed magnetic field distribution is calculated analytically using a perturbation expansion written in terms of a small dimensionless parameter corresponding to the magnetic susceptibility. When the magnetic field is applied perpendicular to the axon, the magnetic field in the intracellular space is not influenced by the myelin, the magnetic field in the myelin sheath oscillates between the fat and water layers, and the magnetic field in the extracellular space just outside the myelin sheath is heterogeneous. This heterogeneity causes the spins to dephase, shortening T_2^*. When the magnetic field is applied along the axon, it is homogeneous within water-filled regions between myelin layers, and therefore the spins will not dephase and the magnetic susceptibility will have no effect on T_2^*. These two solutions predict the perturbed magnetic field distribution in and around an axon arbitrarily oriented in the main magnetic field.

Keywords: Magnetic Resonance Imaging, Myelin, Susceptibility, Myelin Water Imaging, Perturbation.
Section: Mathematical, Physical & Engineering Sciences

1. INTRODUCTION

Magnetic resonance imaging (MRI) has been used to map the myelin water fraction in neural tissue.[3, 11, 16, 18] This technique may be useful for assessing several white matter diseases such as multiple sclerosis,[10] spinal cord injury,[17] and developmental disorders.[4] Typically multicomponent analysis is used to examine the distribution of the longitudinal relaxation time constant T_1, the transverse relaxation time constant T_2, and the experimental transverse relaxation time constant T_2^* in different presumed water pools: free water (with a relatively long T_2^*) and myelin water trapped between layers of the myelin sheath (with a relatively short T_2^*). Measuring the relative fraction of water within the myelin provides information about the degree of myelination of the axons and possibly about normal and abnormal development, dysmyelination, or demyelination.

T_2^* relaxation arises from microscopic perturbations in the magnetic field that cause the spins to dephase. One source of these perturbations is a heterogeneous distribution of magnetic susceptibility. Interest in magnetic susceptibility imaging is growing,[6] and it is becoming an important contrast mechanism in MRI,[7, 8, 13–15, 19] particularly for studying white matter in the brain.[21–23]

To determine the impact of a heterogeneous susceptibility distribution in and around an axon, we must solve

*Author to whom correspondence should be addressed.
Email: roth@oakland.edu

a partial differential equation for the resultant perturbed magnetic field. This calculation requires consideration of multiple spatial scales: from the individual layers of myelin surrounding the axon (nanometers) to the radius of the axon itself (microns) to the voxel size in a magnetic resonance image (millimeters). Because the susceptibility is small, perturbation methods are appropriate. In this paper, our hypothesis is that local perturbations in the magnetic field arise because of different magnetic susceptibilities in myelin and water. We calculate the resulting perturbed magnetic field distribution and estimate how this field will affect T_2^*, including its orientational dependence (that is, its anisotropy).

2. MODEL

Because the length of a typical axon is so much greater than its diameter, we approximate it as an infinitely long, straight cylinder and indicate position using cylindrical coordinates $(r,\ \theta,\ z)$ centered on the axon. The central core of the cylinder $r < a$ represents the intracellular space (mostly water) with magnetic permeability μ_o. The region outside of the cylinder, $r > b$, represents the surrounding extracellular space, also with permeability μ_o. We model the magnetic permeability of the myelin sheath, consisting of alternating myelin layers and intramyelin water layers in the region $a < r < b$, by an oscillating function of r

$$\mu = \mu_o\left[1+\frac{\chi}{2}(1-\cos(k(r-a)))\right] \tag{1}$$

where χ is the magnetic susceptibility of the myelin and k is the spatial frequency corresponding to the individual layers of myelin making up the sheath. To ensure that the permeability is continuous at $r = b$, we require that $k(b-a) = 2\pi n$, where n is the number of layers of myelin (a large integer, on the order of 100). The susceptibility is a dimensionless number with a magnitude on the order of 10^{-5} in biological tissue, making it an ideal perturbation parameter.

Because no free current is present, the curl of the magnetic H-field is zero, $\nabla\times\mathbf{H} = 0$. This allows us to write $\mathbf{H}$ in terms of a scalar magnetic potential, $\mathbf{H} = -\nabla\phi$ [9] We assume the myelin is a linear medium so that the magnetic field, $\mathbf{B}$, is related to $\mathbf{H}$ by $\mathbf{B} = \mu\mathbf{H}$. Since the magnetic field is divergenceless ($\nabla\cdot\mathbf{B} = 0$), the differential equation we need to solve is

$$\nabla\mu\cdot\nabla\phi + \mu\nabla^2\phi = 0. \tag{2}$$

Because the magnetic permeability varies only in the radial direction, Eq. (2) becomes

$$\frac{\partial\mu}{\partial r}\frac{\partial\phi}{\partial r} + \mu\left[\frac{1}{r}\frac{\partial}{\partial r}\left(r\frac{\partial\phi}{\partial r}\right)+\frac{1}{r^2}\frac{\partial^2\phi}{\partial\theta^2}\right] = 0. \tag{3}$$

Here we are assuming the magnetic susceptibility within each myelin layer is isotropic.

Our goal is to find the scalar magnetic potential, ϕ, that obeys Eq. (1) and results in a magnetic field that is continuous (implying that ϕ and its radial derivative should be continuous) at $r = a$ and b. $\mathbf{B}$ should equal the applied magnetic field $\mathbf{B}_o$ for $r \gg b$.

3. RESULTS

CASE 1: *The applied magnetic field is perpendicular to the axon.*

We assume that a uniform magnetic field is applied in the x-direction ($\mathbf{B}_o = B_o\ \mathbf{i}$), so that far from the axon ϕ approaches $-(B_o/\mu_o)r\cos\theta$. To find an analytical solution, we will use perturbation theory in the small parameter χ. The scalar magnetic potential has the form $\phi = f(r)\cos\theta$, and we expand $f(r)$ as

$$f(r) = f_0(r) + \chi f_1(r) + \chi^2 f_2(r)\ldots. \tag{4}$$

We then insert Eqs. (1) and (4) into Eq. (3) and collect like powers of χ. We only solve for the 0th- and 1st-order solutions. The equation for $f_0(r)$ is Laplace's equation

$$\frac{1}{r}\frac{d}{dr}\left(r\frac{df_0}{dr}\right) - \frac{f_0}{r^2} = 0 \tag{5}$$

and the equation for $f_1(r)$ is

$$\frac{1}{r}\frac{d}{dr}\left(r\frac{df_1}{dr}\right) - \frac{f_1}{r^2} = -\frac{\mu_0 k}{2}\sin(k(r-a)) \tag{6}$$

in the myelin and Laplace's equation inside the axon and in the surrounding tissue. The solution to the 0th-order equation is just the applied magnetic field. The solution to the 1st-order equation is found by matching boundary conditions. The full solution (to both 0th- and 1st-order equations) is

$$\phi = -\frac{B_o}{\mu_o}r\cos\theta \quad r < a \tag{7}$$

$$\phi = -\frac{B_o}{\mu_o}r\cos\theta\left\{1-\frac{\chi}{4}\left[1-\frac{k^2a^2-2}{k^2r^2}-\frac{2}{kr}\sin(k(r-a))\right.\right.$$
$$\left.\left.-\frac{2}{k^2r^2}\cos(k(r-a))\right]\right\} \quad a < r < b \tag{8}$$

$$\phi = -\frac{B_o}{\mu_o}r\cos\theta\left\{1-\frac{\chi}{4}\left[\frac{b^2-a^2}{r^2}\right]\right\} \quad r > b. \tag{9}$$

Of particular importance for determining the impact on T_2^* is the magnetic field B_x parallel to $\mathbf{B}_o$ (in the x-direction), which influences the spin precession frequency

$$B_x = B_o \quad r < a \tag{10}$$

$$B_x = B_o\left\{1+\frac{\chi}{4}\left[1-\cos(k(r-a))+\cos 2\theta\right.\right.$$
$$\times\left(\cos(k(r-a))-\frac{k^2a^2-2}{k^2r^2}\right.$$
$$\left.\left.\left.-\frac{2}{kr}\sin(k(r-a))-\frac{2}{k^2r^2}\cos(k(r-a))\right)\right]\right\}$$
$$a < r < b \tag{11}$$

$$B_x = B_o\left\{1+\frac{\chi}{4}\cos 2\theta\left(\frac{b^2-a^2}{r^2}\right)\right\} \quad r>b. \tag{12}$$

Often the perturbation of the magnetic field is expressed as $E=(B_x-B_o)/B_o$, which is the same as the fractional shift of the Larmor frequency in the MR signal.[23] In that notation the fractional frequency shift is

$$E=0 \quad r<a \tag{13}$$

$$E=\frac{\chi}{4}\Bigg[1-\cos(k(r-a))+\cos 2\theta \times\left(\cos(k(r-a))-\frac{k^2a^2-2}{k^2r^2}-\frac{2}{kr}\sin(k(r-a))-\frac{2}{k^2r^2}\cos(k(r-a))\right)\Bigg] \quad a<r<b \tag{14}$$

$$E=\frac{\chi}{4}\cos 2\theta\left(\frac{b^2-a^2}{r^2}\right) \quad r>b. \tag{15}$$

Inside the axon ($r<a$), the magnetic field is equal to the applied magnetic field B_o; the susceptibility of the myelin has no effect on the intracellular space. Within the myelin sheath the expression is complicated. However, we can simplify it by noting that there are generally many layers of myelin ($n\gg 1$), so that $kb\gg 1$, in which case the expression for the fractional frequency shift reduces to

$$E\approx\frac{\chi}{4}\ 1-\cos(k(r-a))+\cos 2\theta\ \ \cos(k(r-a))-\frac{a^2}{r^2} \quad a<r<b. \tag{16}$$

Recall that the terms oscillating in r represent myelin for $\cos(k(r-a))\approx -1$ and myelin water for $\cos(k(r-a))\approx 1$. Therefore, in the water-filled spaces between myelin layers we can set the cosine equal to one and Eq. (16) reduces to

$$E\approx\frac{\chi}{4}\cos 2\theta\left(1-\frac{a^2}{r^2}\right), \quad a<r<b. \tag{17}$$

Near the inner surface of the myelin sheath ($r=a$), the heterogeneity vanishes. Near the outer surface ($r=b$), the heterogeneity is proportional to $(b^2-a^2)/b^2$. Rushton[20] and others reported scaling relationships for myelinated axons, such as $a=0.61b$, which implies that $(b^2-a^2)/b^2=0.63$. Therefore, the heterogeneity in the myelin water is approximately $0.16\chi\cos 2\theta$. The factor of $\cos 2\theta$ implies that the frequency shift has a different sign in the direction along the applied magnetic field ($\theta=0$, 180°) than in the direction perpendicular to it ($\theta=90°$, 270°). Lee et al.[12] estimate that the difference between the susceptibility of water and myelin is on the order of -0.10×10^{-6}, implying that these heterogeneity effects should be on the order of one hundredth of a part per million (ppm).

The myelin structure also influences the magnetic field outside the axon. In the nearby surrounding tissue, the magnetic field heterogeneity is as large as in the myelin water near $r=b$, but because the total amount of extracellular water should be large compared to the amount of myelin water (there is no myelin there taking up much of the volume), the T_2^* value may be determined as much by water outside surrounding the axon as it is by water trapped between myelin layers.

Figure 1 shows the magnetic field B_x as a function of position within and surrounding the axon. The applied magnetic field is horizontal, and the plot is of $(B_x-B_o)/(B_o\chi)$. The magnetic field oscillations are most apparent where the myelin layers run parallel to the applied magnetic field (90° and 270°), and the oscillations disappear where the myelin layers lie perpendicular to the field (0° and 180°). The oscillation of the magnetic field is most clearly seen in the highly magnified panels. Realize that the white layers (where the magnetic field is largest) correspond to layers of myelin, whereas the darker regions

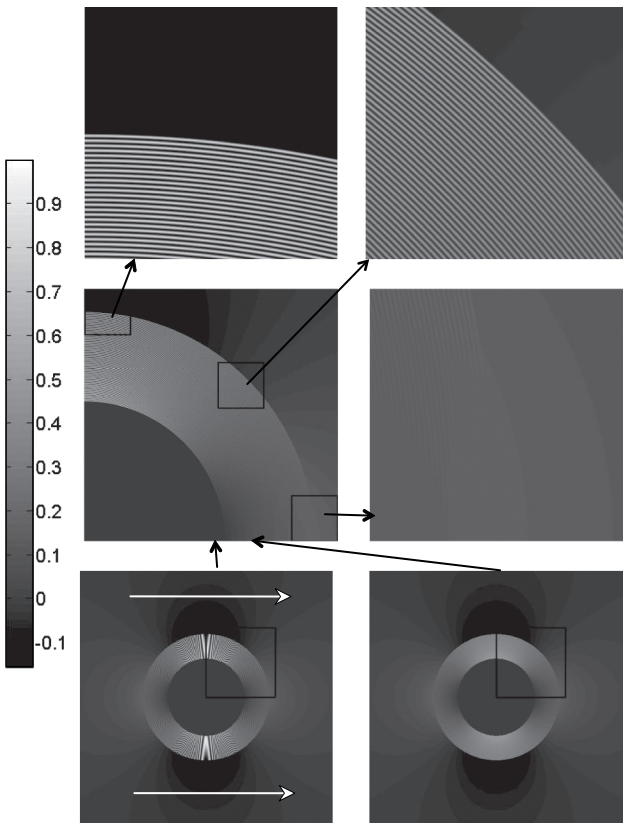

Fig. 1. $(B_x-B_o)/(B_o\chi)$ as a function of position in and around a myelinated axon, calculated using Eqs. (13)–(15). The applied magnetic field is horizontal (white arrows). The lower left plot shows the entire axon cross-section and regions surrounding the axon. The high spatial frequency of the myelin layers ($n=100$) cannot be resolved, and results in severe aliasing in the image. The lower right panel shows the same picture with the myelin oscillations averaged out, eliminating the aliasing. The middle left panel shows a magnified view of one quadrant of the axon; some minor aliasing is still apparent. The top two panels and the middle right panel show further magnified views of the myelin, indicating the magnetic field oscillations in the myelin layers.

(where the magnetic field is smaller) correspond to water between myelin layers. If only water is being imaged, the heterogeneity is somewhat less dramatic than it appears in Figure 1.

CASE 2: *The applied magnetic field is parallel to the axon.*

The magnetic field parallel to the fiber axis ($\mathbf{B}_o = B_o\mathbf{k}$) is a trivial case, for which we can find an exact solution without resorting to perturbation theory. All equations are satisfied and boundary conditions are met if the H-field is simply equal to $H_o = B_o/\mu_o$, and $B = \mu H_o$, where μ is equal to μ_o inside and outside the axon and is given by Eq. (1) in the myelin. Therefore, the magnetic field varies throughout the myelin sheath, but in the regions of water between myelin layers ($\cos(k(r-a)) = 1$) the magnetic field is simply the applied field B_o, implying that the fractional frequency shift is zero and the myelin susceptibility should not contribute to T_2^*.[8]

4. DISCUSSION

We calculate the perturbed magnetic field in and around a myelinated axon in the presence of an applied magnetic field, taking into account the magnetic susceptibility of the myelin. By using perturbation theory, we find an analytical solution that predicts how the magnetic field depends on the model parameters. Several conclusions arise from our analysis. When the magnetic field is applied perpendicular to the axon, we find that:

(1) the magnetic field in the intracellular space is not influenced by the myelin, so the spins within the axoplasm all precess at the Larmor frequency;

(2) the magnetic field in the myelin sheath oscillates between the lipid and water layers, and in the water layer the magnetic field is heterogeneous so that spins in water trapped between myelin layers precess at a frequency higher than the Larmor frequency at locations along the applied magnetic field, but at a frequency lower than the Larmor frequency at locations perpendicular to the applied field; this effect is more pronounced near the outer layers of the myelin ($r = b$) compared with the inner layers ($r = a$); and

(3) the magnetic field in the extracellular space just outside the myelin sheath ($r > b$) is also heterogeneous, so that extracellular spins also precess with a heterogeneous distribution of frequencies, causing the spins to dephase more rapidly, shortening T_2^*.

If the magnetic field is applied along the axon, the magnetic field is homogeneous within water-filled regions, and therefore the spins will not dephase and the magnetic susceptibility will have no effect on T_2^*.

In general, a magnetic field applied at an angle with respect to the axon's axis can be decomposed into parallel and perpendicular components, in which case the resultant field distribution can be found as a linear superposition of the two cases analyzed above.

Our result reduces to what one finds by modeling the myelin sheath as a uniform cylinder with average susceptibility $\chi/2$, if we average our results over the sheath by ignoring the oscillating terms in Eq. (14) and assuming that $kb \gg 1$. Equation (14) for the fraction frequency shift in the myelin becomes

$$E \approx \frac{\chi}{4}\left[1 - \frac{a^2}{r^2}\cos 2\theta\right] \tag{18}$$

This result is not the same as Eq. (17), found by evaluating the fractional frequency shift experienced by the myelin water. The two equations are equal for $\theta = 0$, but differ at other angles. Our model and the uniform susceptibility model also differ if the magnetic field is parallel to the axon, in which case the uniform average susceptibility model will predict a frequency shift experienced in the myelin, whereas our model predicts no frequency shift experienced by the myelin water. Therefore, the uniform susceptibility model for the myelin sheath incorrectly predicts the spatial distribution of the fractional frequency shift experienced by the myelin water. The oscillating nature of the susceptibility distribution is crucial to obtain the correct result.

Our model has several limitations. First, we consider only a single axon, but a nerve bundle or fascicle typically consists of many axons. A more detailed study is needed to predict the magnetic field perturbation in and around a closely spaced "pack" of axons, accounting for interactions between them. To a first approximation, the influence of the surrounding axons can be accounted for using a Lorentz cavity,[5] but this may be too simple an approximation for the complex structure of white matter. Second, we assume that the susceptibility oscillates sinusoidally across the myelin sheath. This was the approximation that allowed us to obtain an analytical solution. An alternative assumption would be to take the susceptibility as varying piecewise, alternating between the two values of 1 and χ.[22] Such a calculation requires matching boundary conditions at $2n$ fat-water boundaries, and can result in sums over the myelin layers in the resulting expressions. Such methods have been proposed by Burridge and Keller[2] and used by Basser[1] in a composite model of myelinated axons. Our assumption of a sinusoidal dependence can be thought of as the first term in a Fourier series representation of the susceptibility distribution, and we expect that it captures the first-order behavior resulting from a spatially oscillating susceptibility. Third, we assume that the axon is long and straight; this assumption will not be satisfied if axons undulate or if we consider large enough spatial scales where fascicles may splay, converge, twist or bend, but we believe this is a good approximation over short distances. In addition, there are nodes of Ranvier punctuating long lengths of myelin insulation in these axons. These nodes are also deemed to have a negligible effect on the microscopic variation of the magnetic field because they appear approximately

once every 100 axon diameters.[20] Fourth, we assume the magnetic susceptibility of the myelin is isotropic. Myelin has been modeled with an anisotropic susceptibility,[21–23] and our model could be extended to this case. Fifth, we assume the tissue surrounding the axon and axoplasm inside it have a magnetic susceptibility of zero. While this may not be accurate, it is straightforward to repeat the calculation using a different value of susceptibility (perhaps that of water), and the key parameter entering our expressions will be the difference between the susceptibility of water and myelin. Finally, we ignore other factors that may contribute to signal heterogeneity, such as the contribution of protons that are not in water but instead are in the fatty myelin itself, the chemical shift, perturbations caused by blood vessels, differences in diffusion, the chemical exchange of protons between water and macromolecules, etc. A crucial question is if myelin susceptibility contributes more or less than these other factors to a reduction in T_2^*.

5. CONCLUSION

Our analysis shows how myelin water in neural tissue impacts the MRI signal. The calculation uses perturbation theory to account for the multiscale behavior of the tissue. Microscopic heterogeneities of susceptibility reduce the macroscopic T_2^* of the myelin water. For a magnetic field perpendicular to the axon, the fractional shift of the Larmor frequency inside the axon is zero. Within the myelin sheath the frequency shift oscillates between the fat and water layers, and in the extracellular space it is heterogeneous. When the magnetic field is applied along the axon, the susceptibility does not shift the Larmor frequency of the myelin water.

Acknowledgments: This research was supported by the National Institutes of Health grant R01EB008421 (Bradley J. Roth, Steffan Puwal) and by the Intramural Research Program of the *Eunice Kennedy Shriver* National Institute of Child Health and Human Development (Peter J. Basser).

References and Notes

1. P. J. Basser; Cable equation for a myelinated axon derived from its microstructure; *Med. Biol. Eng. Comput.* 31, S87 **(1993)**.
2. R. Burridge and J. Keller; Poroelasticity equations derived from microstructure; *J. Acoust. Soc. Am.* 70, 1140 **(1981)**.
3. S. C. L. Deoni, E. Mercure, A. Blasi, D. Gasston, A. Thomson, and M. Johnson; Mapping infant brain myelination with magnetic resonance imaging; *J. Neurosci.* 31, 784 **(2011)**.
4. S. C. L. Deoni, D. C. Dean III, J. O'Muircheartaigh, H. Dirks, and B. A. Jerskey; Investigating white matter development in infancy and early childhood using myelin water fraction and relaxation time mapping; *NeuroImage* 63, 1038 **(2012)**.
5. C. J. Durrant, M. P. Hertzberg, and P. W. Kuchel; Magnetic susceptibility: Further insights into macroscopic and microscopic fields and the sphere of Lorentz; *Magn. Reson. A* 18, 72 **(2003)**.
6. E. M. Haacke and J. R. Reichenbach; Susceptibility Weighted Imaging in MRI, Wiley, Hoboken, New Jersey **(2011)**.
7. E. M. Haacke, S. Mittal, Z. Wu, J. Neelavalli, and Y.-C. N. Cheng; Susceptibility-weighted imaging: Technical aspects and clinical applications, Part 1; *AJNR* 30, 19 **(2009)**.
8. X. He and D. A. Yablonskiy; Biophysical mechanisms of phase contrast in gradient echo MRI; *PNAS* 106, 13558 **(2009)**.
9. J. D. Jackson, Classical Electrodynamics, 3rd edn., Wiley, New York **(1999)**.
10. H. H. Kitzler, J. Su, M. Zeineh, C. Harper-Little, A. Leung, M. Kremenchutzky, S. C. Deoni, and B. K. Rutt; Deficient MWF mapping in multiple sclerosis using 3D whole-brain multicomponent relaxation MRI; *NeuroImage* 59, 2670 **(2012)**.
11. S. H. Kolind, B. Madler, S. Fischer, D. K. B. Li, and A. L. MacKay; Myelin water imaging: Implementation and development at 3.0T and comparison to 1.5T measurements; *Magn. Reson. Med.* 62, 106 **(2009)**.
12. J. Lee, K. Shmueli, B.-T. Kang, B. Yao, M. Fukunga, P. van Gelderen, S. Palumbo, F. Bosetti, A. C. Silva, and J. H. Duyn; The contribution of myelin to magnetic susceptibility-weighted contrasts in high-field MRI of the brain; *NeuroImage* 59, 3967 **(2012)**.
13. W. Li, B. Wu, and C. Liu; Quantitative susceptibility mapping of human brain reflects spatial variation in tissue composition; *Neuroimage* 55, 1645 **(2011)**.
14. W. Li, B. Wu, A. V. Avram, and C. Liu; Molecular underpinnings of magnetic susceptibility anisotropy in the brain white matter; *Proc. ISMRM*, Melbourne, Australia **(2012)**, Vol. 20, p. 379.
15. C. Liu; Susceptibility tensor imaging; *Magn. Reson. Med.* 63, 1471 **(2010)**.
16. A. MacKay, K. Whittall, J. Adler, D. Li, D. Paty, and D. Graeb; *In vivo* visualization of myelin water in brain by magnetic resonance; *Magn. Reson. Med.* 31, 673 **(1994)**.
17. E. L. MacMillan, B. Madler, N. Fichtner, M. F. Dvorak, D. K. B. Li, A. Curt, and A. L. MacKay; Myelin water and T2 relaxation measurements in the healthy cervical spinal cord at 3.0T: Repeatability and changes with age; *NeuroImage* 54, 1083 **(2011)**.
18. S. M. Meyers, C. Laule, I. M. Vavasour, S. H. Kolind, B. Madler, R. Tam, A. L. Traboulsee, J. Lee, D. K. B. Li, and A. L. MacKay; Reproducibility of myelin water fraction analysis: A comparison of region of interest and voxel-based analysis methods; *Magn. Reson. Imag.* 27, 1096 **(2009)**.
19. E. Özarslan and P. J. Basser; Dependence of the MR lineshape for white-matter on the orientation of the B0 field: Insights from a three-phase model; *11th International Conf. on Magn. Reson Microscopy*, Beijing, China **(2011)**.
20. W. A. H. Rushton; A theory of the effects of fibre size in medullated nerve; *J. Physiol.* 115, 101 **(1951)**.
21. P. Sati, P. van Gelderen, A. C. Silva, D. S. Reich, H. Merkle, J. A. Zwart, and J. H. Duyn; Micro-compartment specific T_2^* relaxation in the brain; *NeuroImage* 77, 268 **(2013)**.
22. A. Sukstanskii and D. A. Yablonskiy; On the role of neuronal magnetic susceptibility and structure symmetry on gradient echo MR signal formation; *Magn. Reson. Med.* 71, 345 **(2014)**.
23. S. Wharton and R. Bowtell; Fiber orientation-dependent white matter contrast in gradient echo MRI; *PNAS* 109, 18559 **(2012)**.